

Position resolution in a Ge-strip detector

Michael Momayezi, XIA¹
William K. Warburton, XIA
Richard Kroeger, NRL²

We have investigated, both experimentally and theoretically, how to reconstruct in three dimensions the interaction positions for γ -rays penetrating into a double-sided Ge cross strip detector. We found that when a suitable geometry is used, the 3D-reconstruction problem can be reduced to three one dimensional ones, which greatly simplifies the task. We report measurements on a 10mm thick detector with 2mm strip pitch, showing that at least 2mm position resolution can easily be achieved perpendicular to the detector plane. While the in-plane resolution is presently limited to the strip pitch we present work on progress in developing algorithms to improve this. This includes in particular the expected effects of the electronics and the interstrip capacitance on the signal shapes. Finally, we present captured waveforms that indicate the possibility of reconstructing more complex events such as Compton scattering.

Keywords: Digital pulse processing, position resolution

1 Introduction

In many applications, involving hard X-ray or γ -ray detection, it is useful or essential to reconstruct all three coordinates of the photon interaction point within the detection volume. Such applications range from medical imaging to the newly proposed γ -ray detector arrays for nuclear physics. In all cases it is desirable that the reconstruction be made with minimal computational efforts. The complexity of the reconstruction problem directly depends on the detector geometry. Large, capped coaxial Ge-detectors with a segmented outer mantle are highly efficient photon detectors, but require solving a complex 3D problem to find the positions of the γ -ray interactions. On the other hand, a double-sided strip detector with narrow strips allows the 3D reconstruction problem to be decomposed into three independent one dimensional ones. This paper investigates position reconstruction in such planar detectors.

2 Theory

In semiconductor detectors the interacting γ -ray creates energetic electron recoils, which in turn generate clouds of electron-hole pairs as they thermalize. The electric field within the detector volume separates these charge clouds and collects the electrons and holes onto anodes and cathodes, respectively. All detector electrodes are kept at constant potential. The electrons and holes will both induce charges on the detector electrodes during the collection process. The induced charge signals, which initially cancel each other, grow as the electron and hole charge clouds separate.

We will approach the problem of signal formation in a semiconductor strip detector in three steps. The first task is to compute the induced charge on a strip by a point charge anywhere in the volume of the detector. The second is to compute the drift field, which transports the charge carriers to their respective electrodes. The third is to simulate the response of the detecting electronics.

2.1 Green's function of a point charge in a detector

In detectors whose strip width and pitch are small compared to their thickness, an appreciable signal will be seen on any strip only after charge carriers have moved into the vicinity of the strip, i.e. are about a strip

¹ X-Ray Instrumentation Associates, www.xia.com

² Naval Research Laboratory

width away from the strip. This phenomenon is commonly referred to as the 'small pixel' effect¹, and it is key to simplifying interaction location problem in an orthogonal-strip detector. First, it produces a time difference between the response of strips on opposite sides of the detector that is easy to translate into a depth-of-interaction measurement. Then, once the depth is known, one can tackle lateral position determinations independently on each side of the double-sided strip detector. Thus a complex 3D problem can be reduced to three much simpler one-dimensional problems.

If one ignores the edge effects due to the finite size of the detector, the electrostatic problem of finding the induced charges on rectangular strips of finite length is not very difficult, provided the strip separations are small compared to the strip widths. Once the charge induced on a strip from a point charge at any position is known, one can derive the signal formation on the strip by using the known electron and hole drift properties in germanium.

The problem of a point charge between two parallel plates of infinite extent can be solved by constructing Fourier series from solutions of the Laplace equation², or by a summation over infinitely many mirror charges. While the Fourier series are mathematically more appealing, the sums over mirror charges are much easier to handle numerically. Though they converge slowly, they lend themselves very well to convergence acceleration schemes³.

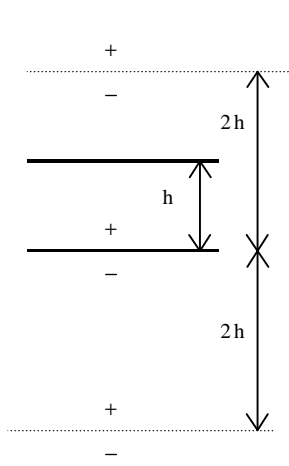


Fig.1: Mirror charges in a planar detector.

The sketch in figure 1 shows the placement and sign of these mirror charges. Note how this arrangement can be viewed as sets of dipoles, pairs of opposite charge carriers, regularly spaced out on a grid with a period of two times the detector thickness. In a rectangular coordinate system the detector is bounded by two planes, at $z=0$ and $z=h$. For a positive charge placed at $z=c$, the center points of the dipoles are located at $\{z_i=2ih\}$ with i ranging from minus to plus infinity. The positive mirror charges are at $z=2ih+c$, the negative ones at $z=2ih-c$.

The contribution from all mirror charges will correctly describe the charge-induced electric fields and potentials anywhere inside the detector and on the inside detector surfaces.

The amount, and sign, of charge induced on any strip is found by integrating the electric field over the surface of the strip and using Gauss' law, $\epsilon E=4\pi\sigma$, where ϵ denotes the dielectric constant, E the electric field and σ the surface charge density.

The area integral can be computed in closed form in Cartesian coordinates for the point charge and each of the mirror charges. The remaining series summation is done numerically.

For the purpose of this work the assumption of a planar detector with infinite extent yields results which are accurate enough for the comparison with signals measured near the detector center. In general, however, it is desirable to take into account that the fields will be distorted at the edges and near the corners of a finite size rectangular semiconductor detector. The construction of the Green's function of a point charge inside an orthorhombic detector exceeds the scope of this paper and will be reported elsewhere.

2.2 Charge collection

For the purpose of this paper we considered charge collection only for the simplified case of a planar detector of infinite extent. We modeled a 1cm thick detector operated at 1500V and we assumed a net impurity concentration, N-type, of $10^{10}/\text{cm}^3$. For the electron and hole drift velocities as a function of the electric field we used the values given by C.Canali et al.⁴ and T.W.Raudorf et al.⁵ Due to the nonlinear relationship between charge carrier velocity and field strength we have solved the carrier transport problem

numerically. It is sufficiently precise in our case to update the velocities at 1ns intervals as the charges move through the crystal.

2.3 Electronics simulation

In the existing experimental setup, the induced charge signals, cf. figure 2, are modified from their ideal shapes. There are two main contributions to this pulse shaping, the finite response time of the preamplifiers and the interstrip capacitance. If the preamplifiers had infinite bandwidth and loop gain, the signals from the strips would look as shown in figure 2, top row. The finite preamplifier bandwidth slows down the signals, while the finite loop gain causes a non-zero input impedance of the integrator. A finite impedance causes dynamic charge sharing between strips during the fast rising edge via the unavoidable interstrip capacitance. This is not true charge sharing as the charge stored on the interstrip capacitance will flow back into the driving channel, leaving no net charge in the spectator channel. However, during the rising edge, the signal forms are distorted on both the driving channel and its neighbor. Hence a simulation has to take both effects into account.

The preamplifiers used in this experiment were one-stage integrators without a subsequent differentiator and pole/zero cancellation stage. They were modeled as one-pole operational amplifiers with a fixed gain-bandwidth product derived from their 10% to 90% rise time in response to a unit step input. The integrator response to the induced charge on a strip was computed by a convolution of the incoming charge signal with the differential (with respect to time) of the unit step response of the preamplifier. This is mathematically equivalent to the more intuitive convolution of the input current (time differential of the charge) with the preamplifier unit-step response. The effect of the interstrip capacitance was taken into account in the same manner.

As can be seen from figure 2 the electronics effects smooth out the ideal charge signal shapes, but the time information is preserved fairly well. The time differences between front and back strip signals spans a range of 213 ns as measured by the electronics, which is a slight compression of the true induced charge time difference span of 250 ns.

3 Experimental setup

We used a 1cm thick double-sided germanium strip detector operated at 1500V bias. Its lateral extent was $50 \times 50 \text{mm}^2$, and it had two orthogonal sets of 25 strips on each side. The strip pitch was 2mm; the separation between strips was $200 \mu\text{m}$. Each strip was instrumented with a room temperature FET and an eV-Products type 603 preamplifier. The boron-implanted p-type strips were in the front and the Li-diffused n-type strips were in the back of the detector.

As a radiation source we used a Co-57 source, which was collimated into a fan beam parallel to the orientation of the front strips. The 4-inch long collimator produced a beam which was $35 \mu\text{m}$ wide at impact and had a divergence of only 0.25mrad. The residual beam at the exit from the 1cm thick detector was therefore only $85 \mu\text{m}$ wide. The 122 keV γ -radiation from Co-57 has an interaction length of 5.75mm in germanium⁶ which allowed us to probe the entire depth of the detector.

The γ -source and collimator were mounted on a computer-controlled platform that could scan the beam across the front strips in steps of $1/1000^{\text{th}}$ of an inch. In this work, we scanned the beam in 0.5mm steps across three front side strips.

We instrumented 4 strips on the detector, 3 in the front and 1 in the back, using a 4-channel digital gamma finder module (DGF-4C) from X-Ray Instrumentation Associates. The device acquired data on an event-by-event basis, including high-resolution energy measurements, time stamping and wave form acquisition as well as immediate pulse shape analysis. It measured waveforms at 40MSPS using a 12-bit ADC⁷.

4 Results

In this section we will show that the depth of interaction can be deduced quite accurately using the differences of arrival times between signal on front and back strips. From there we proceed to show how in-plane position reconstruction, orthogonal to the strips, can be achieved using the induced signals on strips that do not finally collect the main charge, ie which are just spectators.

4.1 Depth of interaction

Figure 2 shows the charge collected on the front and back strip (top row) as a function of time and the preamplifier response to it (bottom row). The left-hand column is for γ -absorption in the front of the detector, while the right-hand column shows the situation for absorption in the rear of the detector. As one can see, the signal time difference between front and back strips for γ -absorption in the front is approximately 113 ns after electronics effects have been taken into account. For absorption in the rear the relative timing between front and back strip is reversed. The bullets on the curves show the time intervals at which a 40 MHz wave form digitizer samples the wave forms.

There is a slight asymmetry in the time difference between front and back conversion, which is due to differences in electron and hole drift velocities and the asymmetric field distribution caused by the space charge in the depleted detector volume. The measured arrival time differences, front minus back, range from -113 ns to 100 ns. These can be used to determine the depth of interaction.

In figure 3 we show a distribution of measured time differences. For this measurement we required a coincidence between any of the three front strips and the back strip. The coincidence window was approximately 400 ns wide. In the analysis we selected only events in which the back strip reported the full photon energy, 122 keV. At the same time one, and only one, front strip was required to have collected 122 keV. The width of the energy cut (± 2 keV) was given by the energy resolution, which ranged from 1.4 keV to 1.8 keV (fwhm) for the different strips. There were no events leading to depth-of-interactions inconsistent with the detector geometry, i.e. the count values outside the -113 ns to $+100$ ns range were zero.

These requirements strongly bias the event selection towards photoconversion. In such events the γ -ray did not interact previously, and the probability of observing the 122 keV photoconversion should fall exponentially with the depth into the germanium crystal. As can be seen in figure 3, the measured data agree very well with this expectation. The measured attenuation length is 5.6 ± 0.6 mm. The attenuation length derived from the total interaction cross section is 5.75 mm⁶.

4.2 Deriving in-plane position from spectator signals

Once the interaction depth is known from the time measurement, it should in principle be possible to obtain more information about the event location in the direction orthogonal to the strip orientation by looking not only at the signal from the charge collecting strip, but also at the signals from its neighboring spectator strips. The spectator strips see a transient signal, the size and shape of which carries position information. Figure 4 indicates the size of this effect. It shows computed spectator signals for photo-conversions occurring underneath the strip center (a) and close to the interstrip gap (b). While spectator signals could be large, with pulse heights up to 50% of the main signal, they are shaped and reduced in amplitude by the preamplifier. Indeed the amplitudes and pulse shapes are strong functions of the preamplifier characteristics and the interstrip capacitance. Very accurate modeling is therefore required to correctly predict the pulse shapes of the spectator signals. There is only a small pulse height difference of 10% of the main signal amplitude for photoconversions occurring underneath the strip center and close to its edge. This difference corresponds to 12 keV for the 122 keV γ -rays from Co-57. In the present setup, the high frequency noise was about 2 keV (rms) while low frequency excursions (500 ns periods) were up to 4 keV. Therefore, in the present setup, the achievable lateral position resolution would be dominated by the electronics noise and probably be limited to a third of a strip width (fwhm).

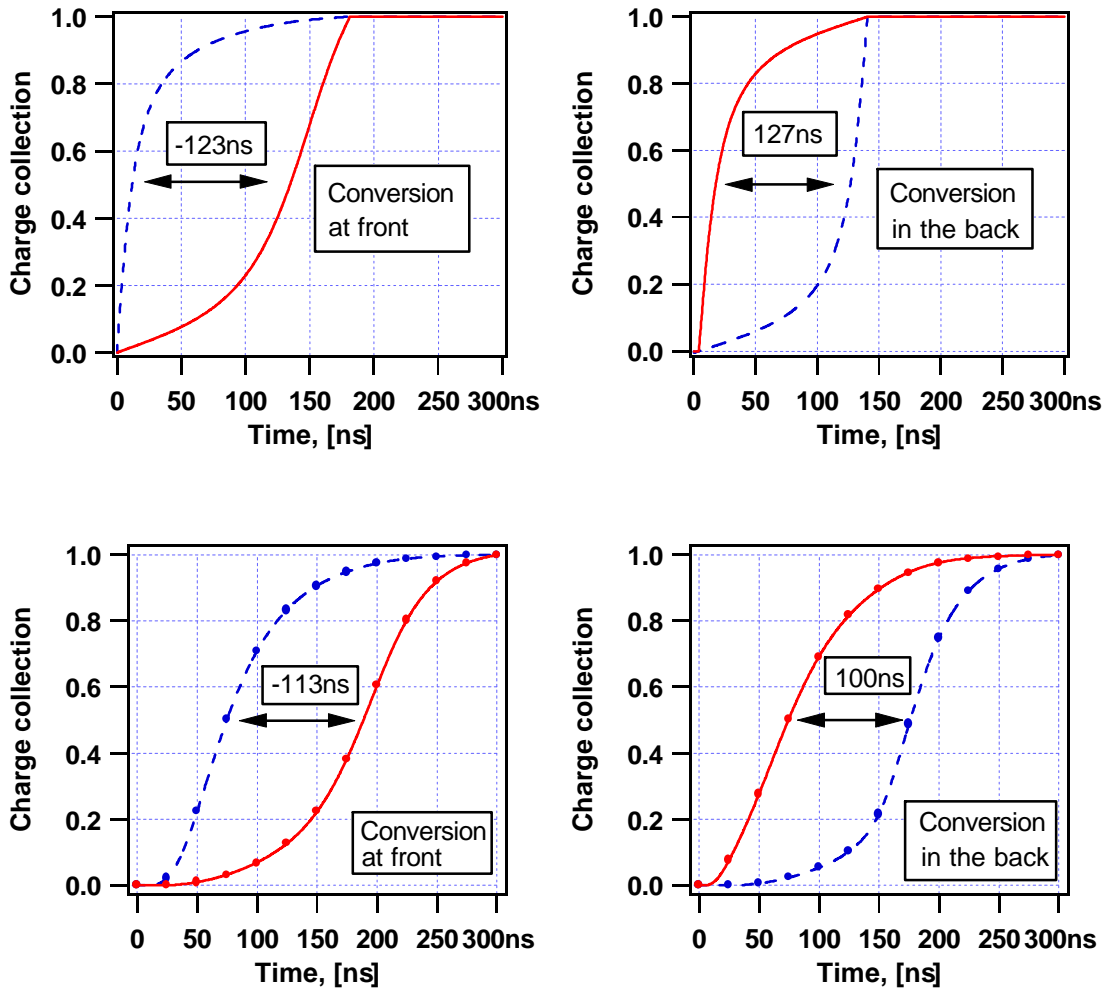


Figure 2: Charge collection onto **front** strip (dashed line) and **back** strip (solid line) for γ -rays converting close to the front (left hand side) or in the back, shown on the right hand side. The top row shows the collected charge as a function of time, i.e. the response of an infinitely fast preamplifier with infinite loop gain; the bottom row shows the response of the real preamplifiers. Note that the time information is well preserved.

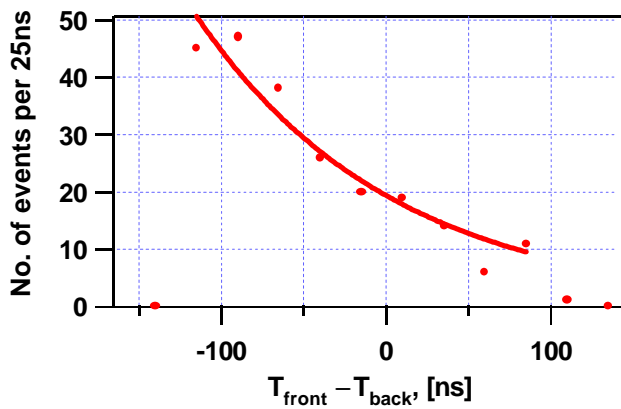


Figure 3: Histogram of measured time differences between front strip and back strip signal. We required 122 \pm 2 keV in any of the three front strips and the back strip. The exponential fit yields an attenuation length of 5.6 \pm 0.6 mm, in good agreement with the NIST value of 5.75mm.

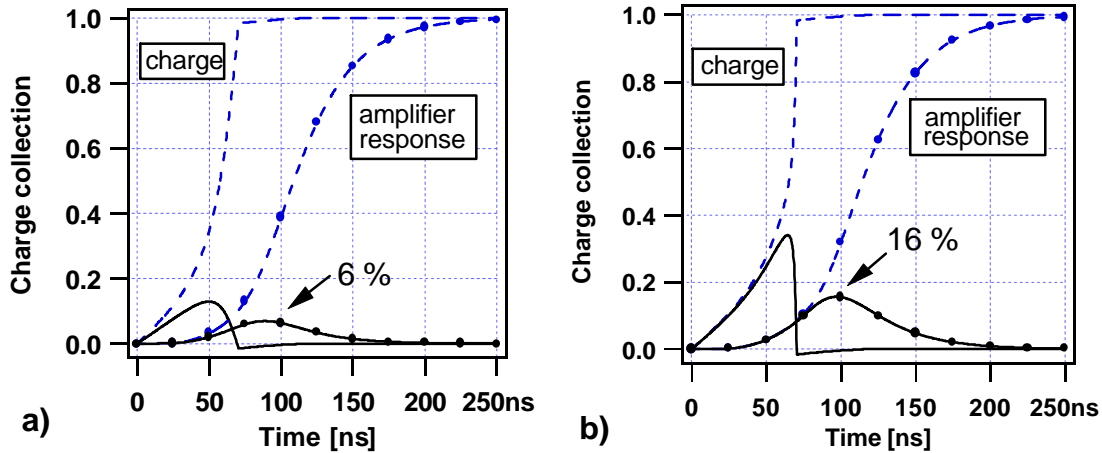


Figure 4: Computed signals in the charge collecting strip (dashed line) and a neighboring spectator strip (solid line). The photoconversion took place in the middle of the detector and underneath the strip center (a) and close to the interstrip gap, (b). Note how the spectator signals are shaped by the preamplifier and reduced in pulse height. The bullets indicate the ADC sampling rate.

To determine whether we could actually achieve this position resolution would have required a larger data set than we were able to acquire in this first experiment. The strong collimation reduced the beam intensity dramatically, and a full day of running produced only about 1000 events with a trigger in any of the front strips and full energy deposition in the back strip. This too small data set prevented us from measuring the achievable position resolution to a reasonable accuracy.

Nevertheless, it was encouraging to observe that the signal wave forms on the collecting strips and the spectators could be reproduced by theoretical computation and electronics simulation using only a small set of assumptions. Figure 5 gives an indication of that.

Here we show signals for photoconversion close to the interstrip gap for different interaction depth, one close to the front (a) and one 7.5mm deep into the detector (b). Note the characteristic negative spectator signal for a conversion close to the boron-implanted front side strips. The signal is negative because the holes were collected quickly and, having traveled only a small distance, they did not induce much charge. The electrons, on the other hand, traverse most of the region where the weighting field of the spectator strip is large. For a photoconversion occurring much deeper than a strip width into the detector, the situation is reversed. Only holes traverse the region of high weighting field of the spectator strip, and consequently the transient signal is positive.

Clearly, the spectator strip pulse shapes carry the information necessary to achieve in-plane position resolutions better than the strip pitch. Suitable algorithms are under investigation.

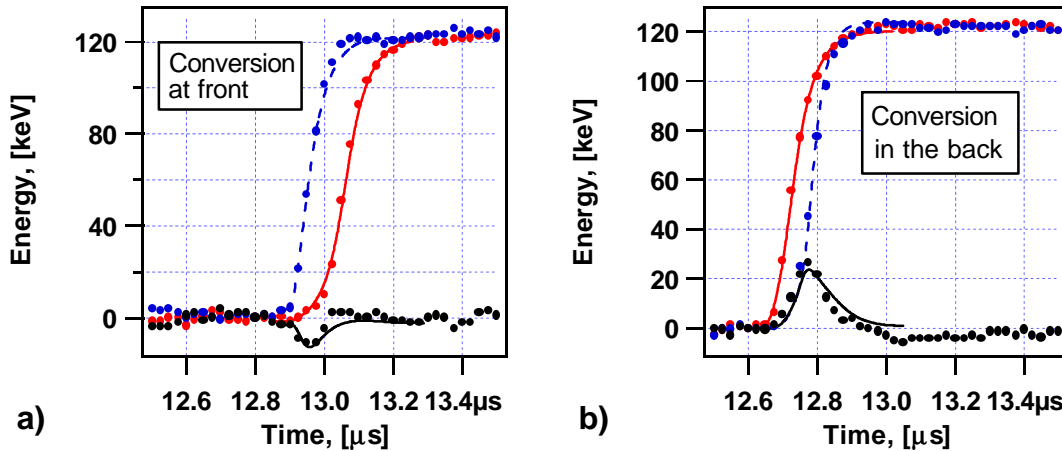


Figure 5: Measured and computed wave forms for photoconversion under the interstrip gap. The conversion occurred close to the front strips (a) and 7.5mm deep into the detector (b). The solid (full energy) line denotes the back strip signal, the dashed line the front strip. Note the transient signals from a spectator strip, during the rise time of the main signals.

4.3 Reconstruction of Compton scattering events

In addition to spectroscopy and imaging uses, a position sensitive germanium detector can also be used for reconstructing more complex events such as Compton scattering. Identifying such events in a multidetector array potentially allows the recovery of γ -ray initial energies, even if they scatter out of one detector and into a second. Being able to make such Compton reconstructions would allow the creation of large arrays of γ -ray detector arrays with very high efficiencies for measuring nuclear reactions which generate high-multiplicity γ -ray bursts.

In figure 6 we show an example of a Compton scattering event, which was completely contained in the instrumented detector region. At 122 keV these events are by no means rare, but account for a third of all interactions. For the event shown, scattering took place close to the interstrip gap between the center and right strip on the front side. The recoil electron acquired 16 keV and dissipated that energy within less than $10\mu\text{m}$ of the initial point of interaction. The scattered photon was absorbed underneath the left-hand strip, where 106 keV were deposited. The scattering angle was 68° with respect to the forward direction. We know the photon was not scattered out of the plane defined by the back strip, because the full energy of 122 keV was collected by that strip.

5 Conclusion

We have shown that in a planar double-sided cross-strip germanium detector it is comparatively easy to obtain 3-dimensional position resolution for the γ -interaction point if time information from front and back side strips is used and the strip widths are small compared to the detector thickness. Being able to measure the depth coordinate of the interaction independently of lateral position allows the decomposition of the 3D position reconstruction problem into three independent one-dimensional problems.

Measuring waveforms and using digital pulse processing for the pulse shape analysis should in principle allow for a lateral position resolution much better than the strip width. We find that a fairly accurate modeling of the detector and preamplifier characteristics will be necessary to correctly predict the pulse shapes, and hence reconstruct the position orthogonal to the strip direction. Further, it will be necessary to substantially reduce the system noise to obtain very fine position resolution.

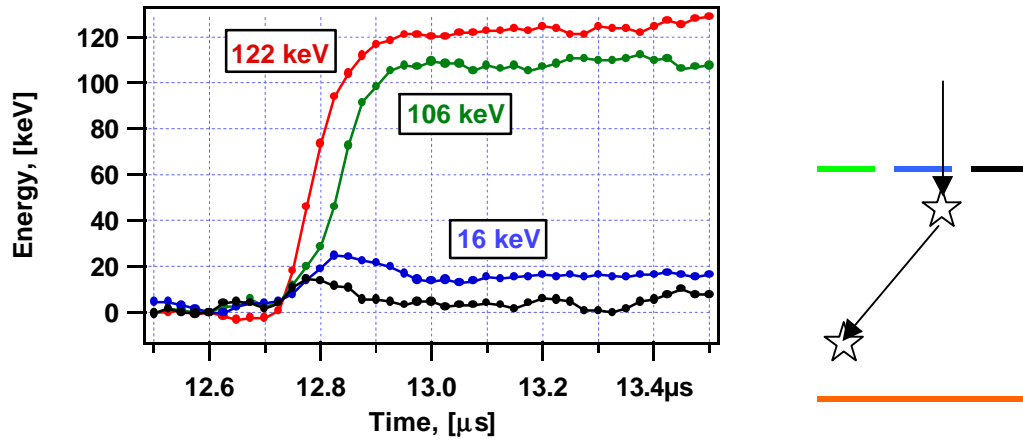


Figure 8: A Compton scattering event. The incoming photon scattered close to the interstrip gap between the right strip (spectator) and the center front strip (labeled 16 keV). The recoil electron received 16 keV. The scattered photon emerged at an angle of 68° with respect to the forward direction and was absorbed under the left strip (labeled 106 keV) where it deposited the remaining 106 keV. The photon was not scattered out of the plane defined by the back strip (labeled 122 keV) as this collected the full energy of 122 keV.

The first data obtained with a strip detector and a highly collimated Co-57 source agreed very well with expectations. Based on this and Warburton's preliminary calculations¹ we believe that we can devise algorithms, simple enough for real time processing, which take wave form data and distill parameter values from them which a computer can easily turn into the position of a γ -interaction in three dimensions.

Acknowledgements

Two of the Authors, W.K.Warburton and M.Momayezi, gratefully acknowledge the support from of the National Institutes of Health, National Cancer Institute through SBIR Grant no. 1-R43-CA75844-01.

References

1. W.K.Warburton, Mat.Res.Soc.Symp.Proc., Vol.487, pp 531-5, 1998
2. J.D.Jackson, "Classical Electrodynamics", 2nd ed., John Wiley and Sons, 1975
3. B.Sarkar, K.Bhattacharyya, Phys.Rev.B, **48**(10), pp.6913-8, 1993
4. C.Canali et al., IEEE-ED, pp1045, Nov.1975
5. T.W.Raudorf, R.H.Pehl, Nucl.Instr.Meth. **A255**, pp538, 1987
6. NIST Standard Reference Database 8 (XGAM), NBSIR 87-3597, XCOM: Photon Cross Section Database, <http://physics.nist.gov/PhysRefData/Xcom/Text/XCOM.html>
7. B.Hubbard-Nelson et al., Nucl.Instr.Meth. **A422**, pp411-6, 1999